Journal of Materials Chemistry B

PAPER

View Article Online
View Journal | View Issue

Cite this: J. Mater. Chem. B, 2014, 2, 4720

Self-assembly and pH response of electroactive liquid core–tetra(aniline) shell microcapsules†

Wei Lv,[a] Jiangtao Feng,[a] Wei Yan*[ab] and Charl F. J. Faul*[c]

Received 12th March 2014
Accepted 13th May 2014

DOI: 10.1039/c4tb00398e

www.rsc.org/MaterialsB

We developed a simple one-pot method to fabricate electroactive tetra(aniline)-based microcapsules, which exhibit a wide range of pH response by self-assembly. In this procedure, the microcapsules are prepared by the facile dialysis-induced self-assembly of tetra(aniline), **TANI**, doped with acetic acid (**HAc**), onto the oil-in-water droplet interface. The chemical structure of the shell is characterized by FT-IR and UV-Vis spectroscopy. The electrochemical properties, self-assembly and pH response of microcapsule dispersions are further investigated by cyclic voltammetry, optical and electron microscopy, dynamic light scattering and aqueous electrophoresis. The size of the microcapsules increases gradually from 1.25 μm to 2.93 μm when the concentration of **HAc** changes from 12 M to 14 M and higher (to become glacial acetic acid). Furthermore, we show that aggregation and stability of the microcapsules can be controlled through changes in pH. This strategy appears to be a general scheme for producing other oligo(aniline)-based microcapsules.

Introduction

Polymer-shell microcapsules with liquid cores have enjoyed considerable success in the applications of active ingredient encapsulation, ranging from food and flavour protection,[1] drug delivery and cell encapsulation[2] to energy storage.[3] The encapsulating techniques and properties of different microcapsules are mainly dependent on the specific shell material with the desired release profile.[4] An interesting area of research within the field of encapsulation focuses on the preparation of microcapsules with a conductive polymer shell.[5] Compared with the common shell materials such as carbohydrates, lipids, and proteins, the attractive advantages of conducting microcapsules are their tuneable optoelectronic properties and capacities of conducting bioelectrical signals, which provides the opportunity to efficiently deliver active ingredients only with electrical stimuli.[5b,c]

As a new class of nanostructured organic (semi)conductors, oligo(aniline)s have drawn increasing academic interest recently. This interest mainly stems from the fact that they: (1) retain the unique redox properties of the polymeric analogue poly(aniline), PANI, and possess relatively high conductivity,[6] (2) possess a well-defined chemical structure and provide molecular engineering possibilities for designing oligo(aniline)-based organic (semi)conductors with defined functionalities and properties,[7] and (3) exhibit good solubility and excellent processability.[8] These attractive advantages of the general class of oligo(aniline) materials have led to increasing interest in developing materials and further applications for these oligomers, including our efforts here to fabricate microcapsules with electroactive shells from the important model compound for PANI, phenyl/amine end-capped tetra(aniline) (**TANI**). Recently, a number of reports have indicated that oligo(aniline)s, as a class of π-conjugated molecules, can self-assemble into well-defined nanostructures and hierarchical microstructures by intermolecular interactions, such as hydrogen bonds, π–π stacking, ionic interactions and hydrophobic interactions.[9]

Specifically, electroactive microcapsules have previously been prepared by self-assembly of **TANI**-based amphiphilic triblock copolymers in solution. Electroactive and acid-responsive vesicles were prepared by self-assembly of the triblock copolymer, $(ANI)_4$-*b*-PEO600-*b*-$(ANI)_4$, synthesized by coupling **TANI**, PEO600 and tolylene-2,4-diisocyanate in aqueous solution.[10] A further electrically switchable vesicle system was prepared by redox-responsive self-assembly of an amphiphilic compound consisting of **TANI** and oligoEO_{10} synthesized by amidation of a leucoemeraldine base (LEB) **TANI** block with oligo(ethylene glycol) monocarboxylic acid.[5b] Unfortunately, the synthesis of copolymer vesicles requires complex procedures, and the attachment of large structural (*i.e.*, functionless) blocks dilutes the electroactive functionality within the bulk material, which is a distinct disadvantage for applications requiring a high density of electroactivity.[6]

[a]Department of Environmental Science and Engineering, Xi'an Jiaotong University, Xi' an, 710049, P.R. China. E-mail: yanwei@mail.xjtu.edu.cn

[b]State Key Laboratory of Multiphase Flow in Power Engineering, Xi'an Jiaotong University, Xi' an, 710049, P.R. China

[c]School of Chemistry, University of Bristol, BS8 1TS, Bristol, UK. E-mail: charl.faul@bristol.ac.uk

† Electronic supplementary information (ESI) available: Characterization, part of the mechanistic study, SEM images of microcapsules prepared using different concentrations of **HAc**, and pH responsive behavior. See DOI: 10.1039/c4tb00398e

Here we present a new strategy for producing electroactive liquid core–**TANI** shell structures in one pot, through a solvent-exchange process in which amphiphilic **TANI** adsorbs onto the oil–water interface and self-assembles into well-defined shells by strong intermolecular interactions. The size of the microcapsules is dependent on the concentration of acetic acid (**HAc**) used in the preparation. The aggregation behaviour and stability of the microcapsules can be controlled through changes in pH.

Experimental

Synthesis

N-Phenyl-1,4-phenylenediamine was purchased from Aldrich Chemical Co. Ltd., and other chemicals were from Tianli Chemical Reagent Co. Ltd. All chemicals were used as received. The synthesis of **TANI** was performed by a modification of the procedure reported in ref. 11. In a typical synthesis, ferric chloride hexahydrate (2.70 g, 10.0 mmol) dissolved in HCl (10 mL, 0.1 M) was quickly poured into a solution of the hydrochloride salt of *N*-phenyl-1,4-phenylenediamine (dianiline salt, 2.56 g, 10 mmol) suspended in HCl solution (50 mL, 0.1 M). After vigorous mechanical stirring for 2 h, the product was collected by centrifugation and washed with 0.1 M HCl repeatedly until the supernatant became clear. The precipitate was purified by Soxhlet extraction with acetone for 12 h to remove any residual dianiline salt. The resulting precipitate was then treated with a mixture of ammonium hydroxide solution (2 M, 50 mL) and acetone (300 mL) for 30 min. The acetone was then removed under reduced pressure. The precipitate was collected by centrifugation and dried in a vacuum oven at 50 °C for 48 h. Characterization of the product is shown in the ESI, Fig. S1.†

Preparation of the electroactive microcapsules

In a typical preparation, 2.0 mg of fine **TANI** powder was dispersed in 4.0 mL of glacial acetic acid and then mixed with 1.0 mL of *n*-octane. The mixture was shaken for 30 seconds and centrifuged at 4000 rpm for 5 min. The supernatant was collected and placed into a dialysis bag (3500 MW cutoff, Viskase). The sealed bag was suspended within a 1 L beaker containing deionized water under stirring to allow the acid to diffuse out of the dialysis bag. The deionized water was replaced every 3 h for 9 h to quickly remove the excess acid until the pH of the deionized water stabilized at 7. The observed small amount of *n*-octane oil suspended at the top of the dialysis bag can be recycled. Calculations (based on average sizes, volumes and wall thicknesses) indicated that the solid content of microcapsules was 6.7 wt%.

Preparation of the microcapsule-modified carbon paste electrode (CPE)

The modified CPE was prepared by thoroughly mixing high purity (99.98%) graphite powder, silicone oil and microcapsule powder in a ratio of 60 : 30 : 10 (w/w) in an agate mortar, using a pestle to obtain a homogeneous paste. A portion of the homogeneous paste was packed into a graphite rod and inserted into a glass tube with $\Phi = 5 \times 1$ mm. A copper wire fixed to the graphite rod and inserted into the glass tube served to establish electrical contact with the external circuit.

Characterization

The formed microcapsules were observed using a L2020 Optical microscope (OM) with a high-resolution optical CCD camera in transmitted illumination mode. A calibration grid with 10 μm spacing was photographed to calculate magnifications. Samples for SEM studies were prepared by depositing 1 to 2 drops of the dispersion onto a piece of concave slide covered with a cover slip. The samples were vacuum freeze dried to prevent the deformation of the spherical shape. SEM images were taken with a JEOL JSM-6700 Field Emission Scanning Electron Microscope. Transmission electron microscopy (TEM) was performed on a JEM model 2100 electron microscope. The samples were prepared by drop-casting 1 to 2 drops of the microcapsule dispersion onto the carbon-coated copper grids and allowed to dry in air. Cyclic voltammetry (CV) was performed on a CHI 660D electrochemical work station with a conventional three electrode cell, using Ag/Ag^+ as the reference electrode and Pt foil as the counter electrode. The prepared microcapsule-modified CPE was used as the working electrode. CV investigations were carried out in 1.0 M H_2SO_4 solutions (degassed for 30 minutes with high purity N_2) in the range from −0.2 to 1.0 V at a scan rate of 50 mV s^{-1}. Dynamic light scattering (DLS) and zeta potential measurements were carried out by using a Malvern Zetasize Nano ZS90 apparatus. FT-IR spectra of the dried samples were obtained on a Bruker, TENSOR37 infrared spectrometer with KBr pellets. Matrix-assisted laser desorption ionization time-of-flight mass spectrometry analysis (MALDI-TOF MS) was performed on an Applied Biosystems 4700 Proteomics Analyzer. UV-Vis spectra were recorded on an Agilent 8453 instrument.

Results and discussion

The as-synthesized **TANI** powder was dissolved in glacial acetic acid and then mixed with *n*-octane. A dispersion of microcapsules with **TANI** as the shell can be formed by dialyzing the mixture against deionized water. Optical microscopy (Fig. 1a) of the resulting dispersion confirmed that microcapsules were formed during the dialysis process. The average diameter of the microcapsules, as determined by measuring 87 particles by SEM, is 2.49 μm ± 0.36 μm (Fig. 1c). This size is slightly smaller than that of hydrodynamic radius determined from DLS (2.9 μm) (Fig. 1b). The broken microcapsules observed in SEM images are evidence for their hollow nature (Fig. 1c as an example). This is further proven by the strong contrast between the dark edge and the pale center in the TEM image (Fig. 1d). The walls of the microcapsules are approximately 50 nm thick. Most of the dry microcapsules (Fig. 1c and d, S2, S6† and 10) are broken (*i.e.*, with one large hole) or have indentations on the surface. The formation of such broken structures may result from solvent evaporation during the vacuum freeze-drying process.[12,13]

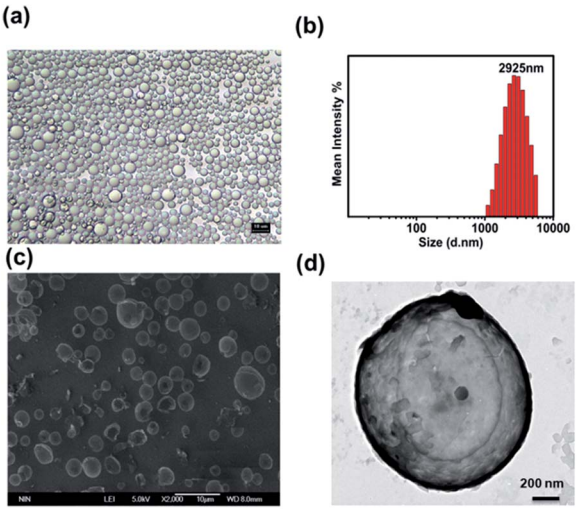

Fig. 1 Typical optical micrograph (a), particle size distribution (b), SEM micrograph (c) and TEM micrograph (d) of the final microcapsules.

TANI as the shell component, which is partly in the **HAc**-doped emeraldine salt (ES) state, is demonstrated by FT-IR and UV-Vis spectra. In Fig. 2, the FT-IR spectra from 1600 to 800 cm^{-1} of the final microcapsules show similar profiles to those observed for the as-synthesized **TANI**. The main peaks at 1599 and 1510 cm^{-1} correspond to C=C stretching vibrations of quinone and benzene rings, respectively. The other bands at 1309, 1167 and 823 cm^{-1} can be assigned to the C–N stretching vibration of a secondary aromatic amine, the aromatic C–H in-plane bending modes, and the C–H out-of-plane bending vibrations of 1,4-aromatic substituted benzene rings, respectively. These peaks are well distinguished in the spectrum of oligo(aniline)s in their emeraldine base (EB) state.[14] However, the dramatic decrease in the ratio of the peak from 1599 to 1510 cm^{-1} emerges in the spectrum of final microcapsules, indicating the presence of doped **TANI**-ES (see Fig. S3†).[7a] Moreover, a relatively strong band at 1662 cm^{-1} observed in the spectrum is also linked to the carboxylic anions as the dopant counterions (see below).[15]

As shown in Fig. 3 (inset), the final blue microcapsule dispersion (b) turns violet when exposed to a base (a) and green when exposed to an acid (c), indicating that the well-known doping/dedoping behaviour of **TANI** occurs, also in the capsules.[16] This phenomenon is in agreement with the unique acid–base doping–dedoping properties of **TANI**. From the UV-Vis spectra, the characteristic absorption maximum observed at 311 nm and 595 nm are ascribed to π–π* transitions of the benzene ring and the benzenoid to quiniod (π_B–π_Q) excitonic transition in **TANI**-EB (Fig. 3a),[7a,9] respectively. Moreover, the main bands at 303, 423 and 786 nm are attributed to the π–π*, polaron–π*, and π–polaron band transitions, respectively. These characteristic absorption peaks are typical for **TANI**-ES (Fig. 3c).[7] As for the UV-Vis spectra of the final microcapsules (Fig. 3b), it exhibits four main peaks located at 317, 421, 595 and 769 nm, among which two bands at 421 and 769 nm are two characteristic absorption peaks in **TANI**-ES and two peaks at 317 and 595 nm are typical for **TANI**-EB. From these data, it can be seen that the **TANI** moieties forming the shell are composed of both **TANI**-EB and **TANI**-ES oxidation states.

Electrochemical properties of microcapsules

CV data shown in Fig. 4 were obtained in 1.0 M sulfuric acid solution with a scan rate of 50 mV s^{-1} in a three-electrode electrochemical cell (as described in the Experimental section). The CV curve obtained from the bare CPE electrode exhibits no obvious peaks, while the CV curve of the microcapsules shows two stronger redox processes. The oxidation peak at 0.321 V corresponds to the LEB to EB transition, while the oxidation peak at 0.571 V shows the transition from the

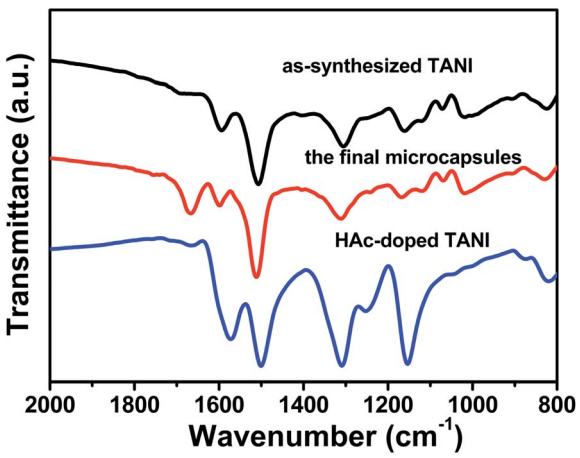

Fig. 2 FT-IR spectra of the as-synthesized **TANI** powder, the final microcapsules and pure **HAc**-doped **TANI**. The characteristic stretching vibrations of **HAc**-doped **TANI**-ES are located at 1570 cm^{-1}(γC=C for quinoid rings), 1493 cm^{-1} (γC=C for benzenoid rings), 1308 cm^{-1} (π-electron delocalization), 1243 cm^{-1} (γC–$N^{+\cdot}$) and 1152 cm^{-1} (γ-NH^{+}=).

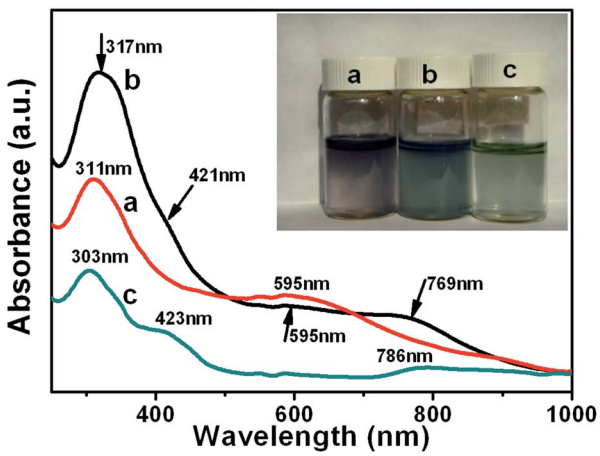

Fig. 3 UV-Vis spectra of the final microcapsule dispersion with the excess *n*-octane oil suspended as the top layer (b), dispersion obtained by dialyzing as-prepared microcapsules with 1 M $NH_3 \cdot H_2O$ (a) and 1 M HCl (c). The inset is a photograph of the corresponding dispersions.

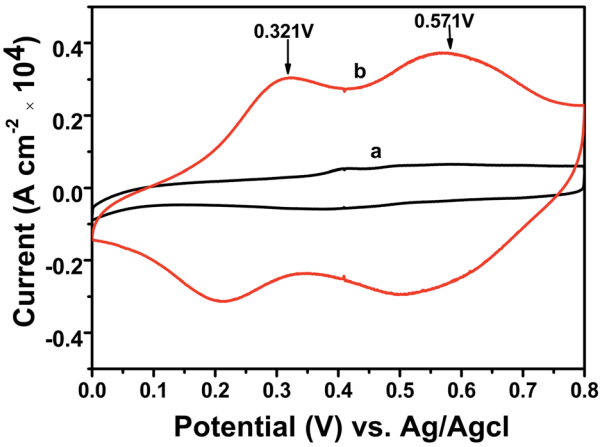

Fig. 4 Cyclic voltammetry of bare CPE (a) and microcapsule-modified CPE (b) in 1.0 M H_2SO_4.

EB state to the pernigraniline base (PB) state, indicating that the **TANI**-based microcapsules show redox activity similar to that expected for simple **TANI** materials.[17]

Proposed formation mechanism of the electroactive TANI-based microcapsules

Fig. 5 schematically shows a possible formation mechanism of the microcapsules. **TANI**-EB is soluble in glacial acetic acid, and can be doped in this environment at the same time. Some of the formed **TANI** in the **HAc**-doped emeraldine salt state, **HAc–TANI**-ES, precipitated from solution because of its lower solubility in glacial acetic acid (see Fig. S4†). In our preparation process, the precipitate was removed and the homogeneous solution placed in the dialysis bag (now containing **TANI**-EB, **HAc–TANI**-ES and *n*-octane oil dissolved in the excess glacial acetic acid, Fig. 5a). During the dialysis process, the excess glacial acetic acid was replaced with water, a non-solvent for both **HAc–TANI**-ES and *n*-octane (which existed as oil droplets in water). Moreover, **HAc–TANI**-ES showed amphiphilic behavior (with hydrophilic –COOH groups from **HAc** and the hydrophobic conjugated backbone), which enabled **HAc–TANI**-ES to bridge the oil droplet–water interface, reducing the total surface energy and acting as a surfactant (Fig. 5b). In order to test this hypothesis, we investigated the influence of the dopant with hydrophilic groups on the formation of microcapsules. Under the same conditions microcapsules were also observed when propanoic acid, β-naphthalene sulfonic acid and dodecylbenzene sulfonic acid were used instead of **HAc** (see Fig. S5†). Driven by π–π stacking interactions, **TANI**-ES molecules can interact with each other to self-assemble into the shell of the microcapsules.[8,10a] In addition, as shown in Fig. 6, the π_B–π_Q absorption of **TANI**-EB is red-shifted by $\Delta\lambda = 16$ nm compared with that of as-synthesized **TANI**. This change indicates that the strong π–π stacking interaction is an important driving force for **TANI** self-assembly into the observed shell structure (Fig. 5c).[9]

Additionally, the electrostatic interactions introduced by the dopants can also serve as a driving force for self-assembly.[7c,8] As shown in Fig. 2, a strong peak located at 1662 cm^{-1}, which can be assigned to the stretching vibrations of the carbonyl group,[14b] exists in the FT-IR spectra of final microcapsules. A likely explanation is that the carboxylic anions are not only acting as dopant counter ions that reside near the positively charged nitrogen atoms, but are also an integral part of the microcapsules (which then also display the characteristic stretching vibrations of carbonyl groups in the FT-IR spectrum). Therefore, the assembly process in this case might also be driven by the electrostatic interactions established between the positively charged **HAc**-doped **TANI** backbone and the excess negatively charged carboxylic anions in a layer-by-layer manner, supported by the thickness of the shell.

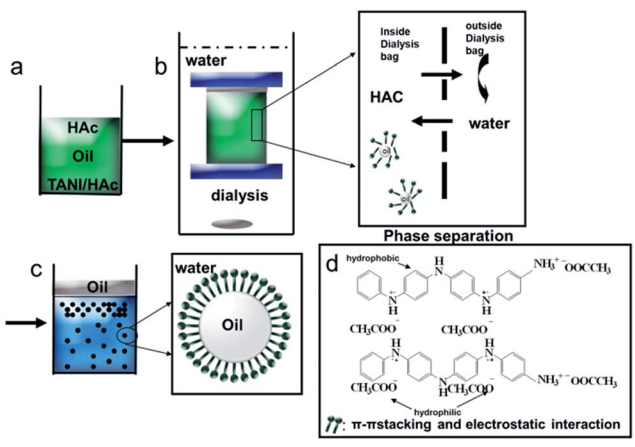

Fig. 5 Schematic of the electroactive liquid core–**TANI** shell microcapsule formation by phase separation induced self-assembly of **TANI** at the oil–water interface.

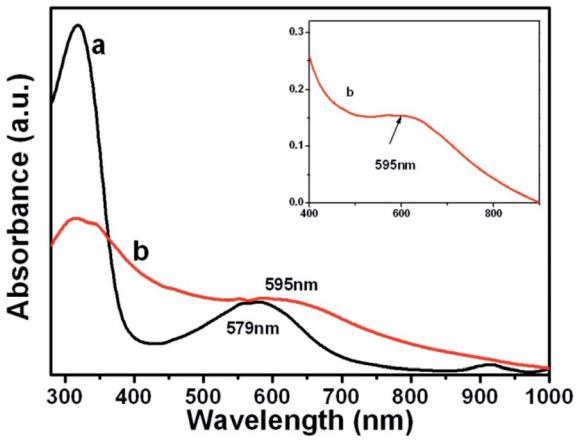

Fig. 6 UV-Vis spectra of (a) as-synthesized **TANI** dissolved in dimethyl sulfoxide without the solvatochromism effect on the π_B–π_Q absorption peak, and (b) **TANI** as the shell in $NH_3 \cdot H_2O$-dedoped EB state microcapsules.

Size control of the microcapsules

The size of the microcapsules can be readily tuned using different concentrations of **HAc** during their preparation (see Fig. 7 and S6†). When 10 M **HAc** is used, hardly any microcapsules are observed, which might be due to insufficient **HAc–TANI**-ES dissolved in the homogeneous phase to form the shell. When 12 M **HAc** is used, microcapsules with an average diameter of 1.28 μm are well dispersed in solution. The average diameter of microcapsules furthermore increased with increased acidity. As the **HAc** concentrations reach 14 M and higher (to become glacial acetic acid when containing no/minimal water), the average diameter of microcapsules increases gradually from 2.44 μm to 2.93 μm. This interesting phenomenon might be attributed to the fact that the higher the **HAc** concentration, the more oil phase dissolves in the **HAc** solution. As the amount of oil phase increases, the number of oil–water droplets increases, which leads to a greater chance of collision between two or more droplets to form larger droplets.[18]

Microcapsules with pH response

Beyond the size control discussed in the previous section, the aggregation behaviour of microcapsules presented in this study are sensitive to pH. As can be seen from Fig. 8, pristine stable microcapsules agglomerate when the pH decreases from 4.8 to 0.8 (addition of HCl) or increases from 4.8 to 13.3 (addition of NaOH). When H_2SO_4 (0.1 M) is used to adjust the pH, agglomerates are also formed (see Fig. S7†). A likely explanation is that the amine groups, found in the chemical structure of the **TANI** shell, are readily protonated below pH 8.[19] Above pH 8 the amine groups are deprotonated, the electrostatic repulsion within the microcapsule particles is weakened, and the particles become unstable. The instability of microcapsules at low pH may be due to the higher ionic strength, causing the electrical double layer around the microcapsules to become more compressed.[20] Aqueous electrophoresis was carried out to confirm the above hypothesis (see Fig. 9). On the one hand, the microcapsules exhibit significant cationic character below pH 9, with the maximum zeta potential observed at around pH 5. On the other hand, the zeta potential decreases with an increase in the conductivity of microcapsule dispersions below pH 5. A likely explanation is that with the decrease in pH with a strong acid such as HCl or H_2SO_4, **HAc** is displaced as a dopant from the **TANI** shell. This process leads to disruption of the assembly of the **TANI** molecules and thus destabilization of the capsules (as observed). A further consequence is the release of **HAc** into the solution (leading to increased ion concentrations, and consequently higher conductivities). However, these postulations are currently under investigation in our laboratories, with the aim of clarifying the nature and origin of these observed changes. These results are in reasonable agreement with the pH-responsive phenomena shown in Fig. 8, and S9.† Thus, stability control of these electroactive microcapsules can be achieved by tuning the pH, which will open up a large range of applications such as polyelectrolyte brushes[21] and 'armoured' microcapsules.[22]

As shown in Fig. 10, microcapsules with diverse organic cores (including octane, heptane, hexane and petroleum ether) can also be prepared by the same method (see also Fig. S9†). These results show that the microcapsules prepared by this simple method have great potential to serve as vehicles for encapsulating hydrophobic (functional) molecules.

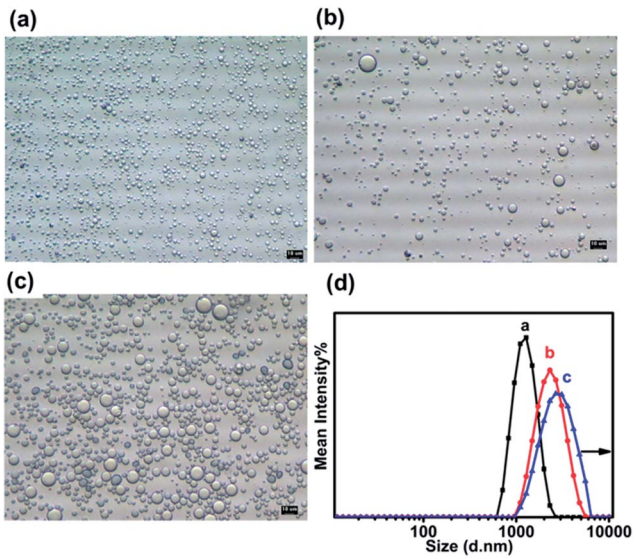

Fig. 7 Optical micrographs and particle size distributions of microcapsules prepared using 12 M HAc (a), 14 M HAc (b) and glacial acetic acid (c) (scale bar = 10 μm).

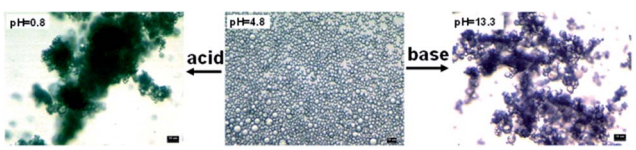

Fig. 8 Optical micrographs of pH-dependent microcapsules at different pH values (adjusted by 0.1 M HCl or 0.1 M NaOH) 1 h after preparation (scale bar = 10 μm).

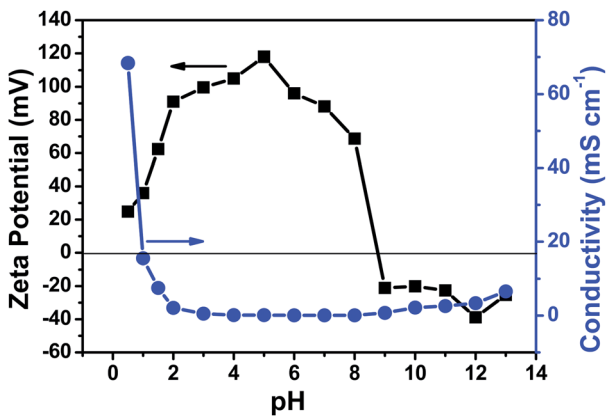

Fig. 9 Zeta potential and conductivity *vs.* pH curves obtained for the suspension of electroactive microcapsules.

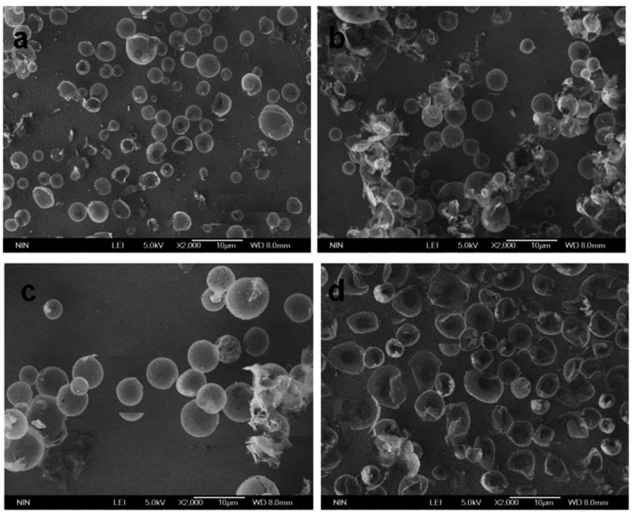

Fig. 10 SEM images of **TANI** microcapsules with *n*-octane (a), *n*-heptane (b), *n*-hexane (c) and petroleum ether (d) as the core.

Conclusions

In summary, we have presented a novel one-pot approach to fabricate electroactive liquid core–**TANI** shell microcapsules suited for encapsulating hydrophobic materials. The size of the microcapsules can be controlled by simple pH changes, with agglomeration of microcapsules triggered when the pH is too low or too high. We believe that such stimulus-responsive microcapsules have potential applications in the broad area of active ingredient delivery, polyelectrolyte brushes, and 'armoured' microcapsules, the areas we are currently exploring with materials other than hydrophobic oils. We are furthermore expanding this approach to other oligo(aniline)-based materials, as shown with the aniline dimer (*N*-phenyl-1,4-phenylenediamine) utilising the same method (see Fig. S10†). Further **TANI**-based materials with complex architectures and aniline oligomers with longer conjugation pathways are currently also under investigation towards the development of further addressable encapsulation approaches.

Acknowledgements

The authors gratefully acknowledge the National Natural Science Foundation of China (Grant no. 21307098), the Fundamental Research Funds for the Central Universities of China, and China Postdoctoral Science Foundation (2013M532053). CFJF acknowledges the University of Bristol for support.

Notes and references

1 Y. Wang, C. P. Su, M. Schulmerich and G. W. Padua, *Food Hydrocolloids*, 2013, **30**, 487.
2 T. Trongsatitkul and B. M. Budhlall, *Langmuir*, 2011, **27**, 13468.
3 (*a*) X. Qiu, W. Li, G. Song, X. Chu and G. Tang, *Energy*, 2012, **46**, 188; (*b*) J. N. Zhang, S. L. Qiu, Y. L. Zhu, Z. Q. Huang, B. B. Yang, W. L. Yang, M. Y. Wu, Q. Y. Wu and J. J. Yang, *Polym. Chem.*, 2013, **4**, 1459.
4 H. N. Yow and A. F. Routh, *Soft Matter*, 2006, **2**, 940.
5 (*a*) C. U. Udeh, N. Fey and C. F. J. Faul, *J. Mater. Chem.*, 2011, **21**, 18137; (*b*) H. Kim, S. M. Jeong and J. W. Park, *J. Am. Chem. Soc.*, 2011, **133**, 5206; (*c*) A. Vimalanandan, L. P. Lv, T. H. Tran, K. Landfester, D. Crespy and M. Rohwerder, *Adv. Mater.*, 2013, **25**, 6980.
6 Z. Wei and C. F. J. Faul, *Macromol. Rapid Commun.*, 2008, **29**, 280.
7 (*a*) Z. Shao, P. Rannou, S. Sadki, N. Fey, D. M. Lindsay and C. F. J. Faul, *Chem.–Eur. J.*, 2011, **17**, 12512; (*b*) Z. Shao, Z. Yu, J. Hu, S. Chandrasekaran, D. M. Lindsay, Z. Wei and C. F. J. Faul, *J. Mater. Chem.*, 2012, **22**, 16230; (*c*) Y. Wang, J. Liu, H. D. Tran, M. Mecklenburg, X. N. Guan, A. Z. Stieg, B. C. Regan, D. C. Martin and R. B. Kaner, *J. Am. Chem. Soc.*, 2012, **134**, 9251.
8 (*a*) Y. Wang, H. D. Tran, X. F. Duan and R. B. Kaner, *J. Am. Chem. Soc.*, 2010, **132**, 10365; (*b*) C. U. Udeh, P. Rannou, B. P. Brown, J. O. Thomas and C. F. J. Faul, *J. Mater. Chem. C*, 2013, **1**, 6428.
9 (*a*) Y. Yan, R. Wang, X. H. Qiu and Z. X. Wei, *J. Am. Chem. Soc.*, 2010, **132**, 12006; (*b*) Y. Zhao, E. Tomsik, J. Wang, Z. Moravkova, A. Zhigunov, J. Stejskal and M. Trchova, *Chem.–Asian J.*, 2013, **8**, 129; (*c*) Y. Zhao, J. Stejskal and J. Wang, *Nanoscale*, 2013, **5**, 2620.
10 Z. Yang, X. Wang, Y. Yang, Y. Liao, Y. Wei and X. Xie, *Langmuir*, 2010, **26**, 9386.
11 W. J. Zhang, J. Feng, A. G. MacDiarmid and A. J. Epstein, *Synth. Met.*, 1997, **84**, 119.
12 U. Jeong, S. H. Im, H. C. Camargo, J. H. Kim and Y. Xia, *Langmuir*, 2007, **23**, 10968.
13 A. Loxley and B. Vincent, *J. Colloid Interface Sci.*, 1998, **208**, 49.
14 (*a*) M. Trchová, I. Šeděnková, E. Tobolková and J. Stejskal, *Polym. Degrad. Stab.*, 2004, **86**, 179; (*b*) Y. Wang, D. H. Tran and R. B. Kaner, *J. Phys. Chem. C*, 2009, **113**, 10346.
15 I. Šeděnková, M. Trchová and J. Stejskal, *Polym. Degrad. Stab.*, 2008, **93**, 2147.
16 D. Li and R. B. Kaner, *Chem. Commun.*, 2005, **26**, 3286.
17 (*a*) Y. N. Xia, J. M. Wiesinger, A. G. Macdiarmid and A. J. Epstein, *Chem. Mater.*, 1995, **7**, 443; (*b*) S. Wang, D. Chao, E. B. Berda, X. Jia, R. Yang, X. Wang, T. Jiang and C. Wang, *RSC Adv.*, 2013, **3**, 4059.
18 W. L. Yan and B. S. Li, *J. Mater. Chem. B*, 2013, **1**, 2525.
19 P. Chambon, A. Blanazs, G. Battaglia and S. P. Armes, *Langmuir*, 2012, **28**, 1196.
20 F. Jin, J. F. Li, X. D. Ye and C. Wu, *J. Phys. Chem. B*, 2007, **111**, 11745.
21 X. Wang, J. Xu, L. Li, S. Wu, Q. C. Chen, Y. Lu, M. Ballauff and X. H. Guo, *Macromol. Rapid Commun.*, 2010, **31**, 1272.
22 R. Chen, D. J. G. Pearce, S. Fortuna, D. L. Cheung and S. A. Bon, *J. Am. Chem. Soc.*, 2011, **133**, 2151.